DOI: 10.24850/j-tyca-2026-05-10

Articles

Spatiotemporal evolution of land use and land cover in the Cuauhtémoc aquifer, Chihuahua

Evolución espaciotemporal de uso de suelo y vegetación en el acuífero Cuauhtémoc, Chihuahua

Miguel Ángel González-Núñez[1], ORCID: https://orcid.org/0000-0002-2952-8787

Humberto Silva-Hidalgo[2], ORCID: https://orcid.org/0000-0002-0628-752X

Adán Pinales-Mungía[3], ORCID: https://orcid.org/0000-0002-1921-7168

María Socorro Espino-Valdés[4], ORCID: https://orcid.org/0000-0002-1232-2774

Miguel Ángel Méndez-Alvarado[5], ORCID: https://orcid.org/0009-0009-4862-1117

Edgar Yuri Mendoza-Cázarez[6], ORCID: https://orcid.org/0000-0001-6916-2428

[1]Universidad Autónoma de Chihuahua-Faculty of Engineering, Chihuahua, Mexico, manunez@uach.mx

[2]Universidad Autónoma de Chihuahua-Faculty of Engineering, Chihuahua, Mexico, hsilva@uach.mx

[3]Universidad Autónoma de Chihuahua-Faculty of Engineering, Chihuahua, Mexico, apinales@uach.mx

[4]Universidad Autónoma de Chihuahua-Faculty of Engineering, Chihuahua, Mexico, mespino@uach.mx

[5]Universidad Autónoma de Chihuahua-Faculty of Engineering, Chihuahua, Mexico, mimendez@uach.mx

[6]Instituto Mexicano de Tecnología del Agua, Jiutepec, Mexico, edgar_mendoza@tlaloc.imta.mx

Corresponding author: Humberto Silva-Hidalgo, hsilva@uach.mx

Abstract

The spatiotemporal distribution of land use and vegetation cover —LULC (best translation approach to Land Use and Vegetation)— in the Cuauhtémoc aquifer, Chihuahua, Mexico, was analyzed using thematic cartography from the National Institute of Geography and Statistics (INEGI), Series I to VII corresponding to the years 1997, 2001, 2005, 2009, 2013, 2017, and 2021. A Geographic Information System (GIS) was used to map, clip, and calculate polygon areas for the seven dates available for these land cover datasets. The vector data are publicly accessible. It was found that in 1997, 36.25 km² (1.06 %) of the aquifer area was used for irrigated agriculture, increasing to 1 016.19 km² (29.79 %) by 2021. In contrast, over the same period, the area covered by oak forest decreased from 116.85 km² (3.42 %) to 104.88 km² (3.07 %). The expansion of agricultural land and the reduction of forested areas coincide with the context of statewide drought and the regional development model, based on agriculture, deforestation of native forest, and the integration of induced grassland. The results indicate the need to pay attention to land use and vegetation changes, such as erosion, desertification, fertilizer-related contamination, and reduced aquifer recharge. The use of drone flights for specific areas, satellite imagery, and GIS is recommended to monitor agricultural land within the aquifer. Understanding the dynamics of LULC change in the aquifer is essential for designing sustainable management strategies that balance agricultural production, water resource conservation, and forest ecosystems in the region.

Keywords: geographical information systems, GIS, land use, vegetation, remote sensing, groundwater, agricultural land, deforestation, desertification, drought, Mexico.

Resumen

Se analizó la distribución espaciotemporal de uso de suelo y vegetación (USV) del acuífero Cuauhtémoc, Chihuahua, México, usando cartografía temática del Instituto Nacional de Geografía y Estadística (INEGI), y series I a VII de 1997, 2001, 2005, 2009, 2013, 2017 y 2021. Se utilizó un sistema de información geográfica para cartografiar, recortar y calcular áreas de polígonos de siete fechas disponibles para estas coberturas. Los datos vectoriales son de acceso público. Se encontró que en 1997, 36.25 km^2 (1.06 %) de la superficie del acuífero se utilizaba para agricultura de riego y en 2021 se incrementó a 1 016.19 km^2 (29.79 %). En contraste, en el mismo periodo se redujo la superficie de bosque de encino de 116.85 km^2 (3.42 %) a 104.88 km^2 (3.07 %). El crecimiento de la superficie agrícola y la disminución de la superficie de bosque coinciden con el contexto de sequía estatal y el modelo de desarrollo regional basado en la agricultura, deforestación del bosque nativo e integración de pastizal inducido. De los resultados, se desprende que se debe prestar atención a problemas de cambio de uso de suelo y vegetación, como erosión, desertificación, contaminación por fertilizantes y reducción de la recarga del acuífero. Se recomienda utilizar vuelos de drones para zonas específicas, imágenes satelitales y SIG para monitorear la superficie agrícola en el acuífero. Es esencial comprender las dinámicas de cambio de USV en el acuífero para diseñar estrategias de manejo sustentable que equilibren la producción agrícola, la conservación de recursos hídricos y los ecosistemas forestales de la región.

Palabras clave: sistema de información geográfica, SIG, uso de la tierra, vegetación, teledetección, agua subterránea, tierra agrícola, deforestación, desertificación, sequía, México.

Received: 31/07/2025

Accepted: 12/01/2026

Available ahead of print: 10/02/2026

Version of record: 01/09/2026

Introduction

Soils constitute a dynamic interface between the lithosphere, atmosphere, and biosphere, playing a critical role in sustaining life and preserving environmental balance. Soil, the main subject of pedology, is a surface layer, has a natural formation process, and is composed of various size solid particles, living matter capable of sustaining vegetation growth and variable water content. It results from the physical and chemical weathering of underlying rocks through processes involving the hydrosphere, atmosphere, and biosphere, which are essential in the formation, development, transport, and deposition of soil (Keller, 2012). Soil comprises organic and inorganic matter and forms a complex terrestrial system. Due to its numerous components, there are many diverse types of soil. Although soil constitutes only a small fraction of the Earth's crust, it is an essential resource for sustaining trophic chains (Tarbuck *et al*., 2020).

As soils support the growth of rooted plants, they form the foundation of the food system upon which humanity depends (Craig *et al*., 2013). They are a natural resource usable through agriculture and are renewable, as they can be preserved and nurtured through crop rotation and fertilizers. However, while soil can be agriculturally productive through irrigation and fertilization, they can also be destroyed or damaged by natural agents or irresponsible human intervention. Human activities such as agriculture, grazing, and rural or urban construction have been introduced into cycle of soil weathering, formation, transport, and erosion, altering the natural processes and their delicate balance, which can be easily disrupted. Therefore, it is much easier for humanity to damage or destroy soils than to create them (Havlin *et al*., 2017; Montiel-González *et al*., 2021; Plaster, 2014; Simental-Nájera *et al*., 2023).

Northern Mexico, like many other regions of the planet, faces significant challenges related to the spatiotemporal distribution of land use and land cover (LULC) change. Some of the problems associated with this topic include desertification, pollution, and soil salinization due to excessive agricultural use among others (Weil & Brady, 2016). Specifically, the Cuauhtémoc Aquifer in Chihuahua, Mexico, has exhibit accelerated changes in LULC since the 20th century, resulting in negative consequences such as erosion, leaching, increased runoff, gullies, and reduced aquifer recharge (Bravo-Peña *et al*., 2016).

LULC studies are conducted for various purposes, including supporting academic and environmental protection programs, planning reforestation activities, supporting habitat conservation programs for animal species, and in the case of this research, preserving agricultural soils for the sustainable development of Mexico. Agricultural soils are a natural resource upon which the growing global population depends, and it is necessary to increase the availability of this resource, even though such availability is continuously decreasing. On a global scale, valuable agricultural soils are being lost due to inadequate conservation measures. For instance, because of land use changes, deserts are expanding worldwide: more than a third of the Earth's surface is occupied by deserts and semi-deserts. Even worse, the productive capacity of vast arid regions in both developed and developing countries is declining alarmingly. Faced with these challenges, tools such as mathematical modeling, artificial intelligence, drone flights and satellite image analysis are also an alternative for LULC studies, beside GIS based assessments.

Mathematical modeling provides a structured framework to simulate hydrological, ecological, and LULC processes, enabling predictive assessments under different scenarios (Taratula *et al*., 2019). Artificial intelligence enhances classification and pattern recognition tasks, improving accuracy in vegetation mapping and LULC change detection (Utami *et al*., 2024). Drone flights allow high-resolution and site-specific data collection, offering high detail in monitoring vegetation health and land surface conditions (Bellia & Lanfranco, 2019). Satellite image analysis ensures broad spatial and temporal coverage, supporting long-term monitoring at local and global scales (Gavade & Rajpurohit, 2021). Finally, GIS acts as an integrative platform, combining spatial datasets from diverse sources to facilitate visualization, overlay, and advanced spatial analyses that support decision-making (Muhangane & Andama, 2024).

Despite these advantages, each method has inherent limitations. Mathematical modeling often relies on simplifying assumptions and requires high-quality input data, which may not always be available. Artificial intelligence methods demand large, well-labeled datasets and can behave as "black boxes", limiting interpretability. Drone flights are constrained by operational costs, weather conditions, and regulatory restrictions, making them less practical for large-scale or continuous monitoring. Satellite image analysis, while extensive in coverage, may be limited by spatial or temporal resolution, cloud cover interference, and high costs for certain datasets.

Due to limitations associated with the previous methods, GIS-based studies are the most widely employed for analyzing LULC change in countries such as Pakistan, India, China, Egypt, Mexico, Nigeria, Poland, and Spain, to name a few (Arif *et al*., 2023; Balogun *et al*., 2011; Hussain *et al*., 2020; López *et al*., 2006; Plieninger, 2006; Shalaby & Tateishi, 2007; Shrestha *et al*., 2021; Wiatkowska *et al*., 2021). Some of the advantages of LULC studies using GIS are their speed, economy and availability of datasets from INEGI for several years in the last decades. A GIS is a set of tools that integrate and relate components that organize, store, manipulate, analyze, and model entities linked to a spatial reference (Chang, 2022; Heywood *et al*., 2010; Slocum *et al*., 2023). GIS tools have been applied in scientific research, natural resource management, hydrology, asset management, archaeology, environmental impact assessment, urban planning, cartography, sociology, historical geography, marketing, surveying, logistics and LULC changes, among others (Antonakos & Lambrakis, 2021; Villanueva-Hernández *et al*., 2019; Xu *et al*., 2021).

When interpreting LULC changes, it is essential to account for potential sources of error that can affect the accuracy of the results. These include: 1) Errors in area calculation, such as inaccuracies arising from projection and conversion processes, the spatial resolution of satellite imagery, and polygon generalization; 2) errors in digitization and polygon delineation, including misclassification in satellite images, inconsistencies in methodologies across different time series, and manual editing mistakes; 3) errors in result interpretation, such as incorrect attribution of change drivers, overestimation of environmental impacts, or comparisons between classes with differing classification accuracy, and 4) uncertainty in reference data, due to the use of datasets from multiple sources or variability in the quality of validation data (Chang, 2016; Heywood *et al*., 2010; Slocum *et al*., 2023). Proper recognition and mitigation of these limitations are crucial to ensure reliable analysis of land cover change.

The objective of this research was to conduct an analysis of the spatiotemporal evolution of LULC in the Cuauhtémoc Aquifer region, located in Chihuahua State, in Northern Mexico, over a 24-year period (from 1997 to 2021). Including: (a) understanding LULC dynamics in the study area (b) estimate the changes in area and percentage of each land cover type, and (c) relate the impact of LULC changes on groundwater availability, particularly considering the increased water extraction, agricultural and urban expansion, and the degradation of natural vegetation. The research findings could be useful to decision making, regulations purposes and management policies in the study area and others showing LULC evolution similarly.

Study area description

Location

The Cuauhtémoc Aquifer is in the west-central region of Chihuahua, Mex., spanning latitudes 28° 14' to 29° 01' N and longitudes 106° 32' to 107° 12' W (Conagua, 2023a). The Cuauhtémoc Aquifer surface area is 3 410.86 km², representing 1.3 % of Chihuahua's territory. It borders the Santa Clara, El Sauz-Encinillas, Alto Río San Pedro, Laguna de Mexicanos, Baja Babícora, and Guerrero-Yepómera aquifers. Geopolitically it covers 85 % of the Cuauhtémoc municipality and partially extends into Guerrero, Bachíniva, Carichí, Cusihuiriachi, and Riva Palacio (Figure 1). The region's primary economic activities include agriculture, livestock farming, commerce, and the production of agricultural equipment, furniture, and dairy products. Large-scale apple production is particularly notable, while other crops include maize, wheat, barley, oats, forage grass, and vegetables (INEGI, 2010).

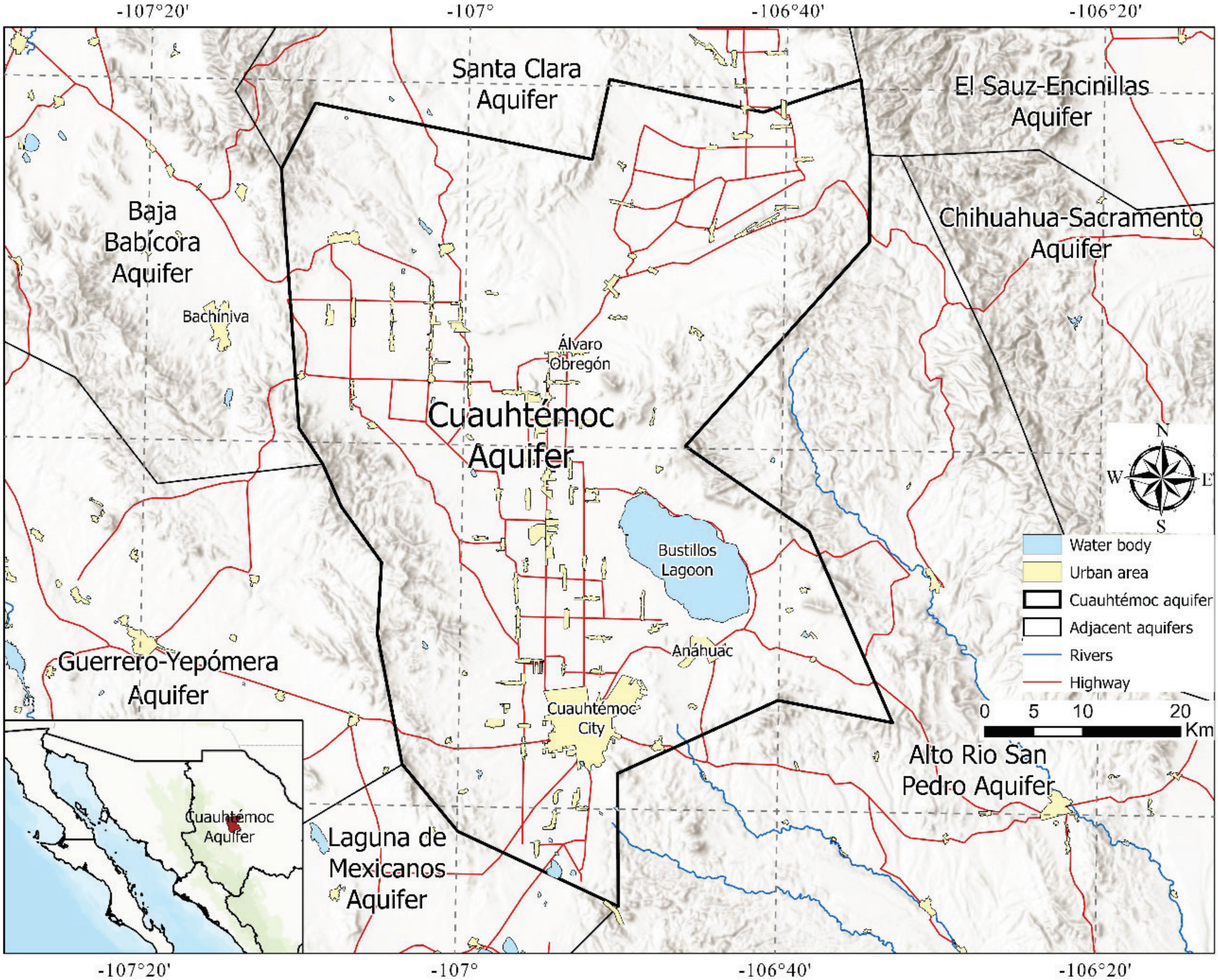

Figure 1. Cuauhtémoc aquifer location including toponymic features (constructed from Conagua, 2026; INEGI, 2025).

Hydrography

The Cuauhtémoc aquifer is in Hydrological Region 34, Northern Closed Basins, within the Northern Closed Basins Subregion and the Laguna Bustillos-Laguna Mexicanos Basin (INEGI, 2010). The drainage network in the basin has a radial pattern, being concentric around the Bustillos Lagoon (Alatorre *et al*., 2019). In the northeastern part of the basin, small intermittent lagoons indicate a flat topography with poor rainwater drainage (Conagua, 2020). The primary inflow to Bustillos Lagoon comes from La Quemada Stream, with 65 km longitude from its origin to the discharge into the lagoon. Additional contributions come from Bustillos Stream and San Antonio Stream, the last crossing through Ciudad Cuauhtémoc before reaching the lagoon. Bustillos Lagoon spans 16 km^2, measuring an average of 8 km in length, 2 km in width, and 2.5 m in depth, at an elevation of 1 975 masl (Conagua, 2020). The region has limited hydraulic infrastructure for managing surface runoff (SGM, 2002).

Climate

The aquifer has a temperate semi-arid climate, classified as BS1, according to Köppen climate classification, adapted to Mexico by Enriqueta García (García, 2004), characterized by hot summers and an average annual temperature ranging from 12 to 18 °C (INEGI, 2010). Within the study area, two climatic variants are identified: BS1 kw (x') and BS1 kw, differing in their winter rainfall distribution. The BS1 kw (x') subtype exhibits a summer rainfall regime (SGM, 2005), while the BS1 kw subtype has both summer and winter rainfall (Conagua, 2023a; SGM, 1997).

In this general climate context, it is important to consider the potential effects of climate change on the regional scale. Previous studies (IMTA, 2015) published projections for the state of Chihuahua, indicating modifications in precipitation and temperature patterns for both a near-term period (2015-2039) and a long-term period (2075-2099). Regarding precipitation, in the near-term period, RCP6.0 scenario, a reduction of 15 % is expected for the spring–summer season. In the long term, all scenarios project a decrease. The pessimist scenario, RCP8.5, indicates a decrease in rainfall of 8.5 % in spring–summer and 10.2 % in autumn–winter (IMTA, 2015).

In terms of temperature, projections show Chihuahua among the states expected to experience the greatest increases. For maximum temperature, the near-term period, RCP8.5 scenario, anticipates increases of +1.6 °C in autumn–winter, while in the long-term period, RCP8.5 scenario, increases of +5.4 °C in spring–summer and +5.5 °C in autumn–winter (IMTA, 2015). Similarly, regarding minimum temperature, Chihuahua is also among the states projected to undergo the most pronounced increases. For the near-term period, RCP8.5 scenario, increases greater than +1.6 °C are expected, and in the long-term period, RCP8.5 scenario, increases of +4.9 °C in spring–summer and +4.4 °C in autumn–winter were projected (IMTA, 2015).

At aquifer level, previous studies (Conagua, 2015) reported an average annual precipitation of 532.3 mm and an average annual temperature of 13.2 °C for the period 1976–2012. More recent data (Conagua, 2023a) confirm similar values for both precipitation and temperature. Other climate studies (Medina-García *et al.*, 2011; SMN, 2025) have documented an increase in local temperature in the

Cuauhtémoc region, which may be linked to higher evapotranspiration rates and intensified groundwater extraction for consumptive uses (UNESCO, 2022).

Pedology

According to pedology studies, Cuauhtémoc Aquifer exhibits three main soil types: Feozem, Regosol, and Cambisol (INEGI, 2010). *Feozem* (92.5 % of the aquifer) is composed of unconsolidated materials such as glacial deposits and loess. Found in humid climates with a distinct dry season, it ranges from warm to wintry conditions, covering temperate zones and tropical highlands. These fertile soils support a variety of rain-fed and irrigated crops, as well as pastures. However, they are prone to flooding and erosion (INEGI, 2014).

Regosol (4.6 % of the aquifer) develops in unconsolidated fine texture materials and is a common soil type across diverse climatic zones and altitudes, particularly in arid regions, dry tropics, and mountainous areas. Its primary use is extensive grazing with low stocking rates under irrigation (INEGI, 2014). *Cambisol* (2.7 % of the aquifer) develops on altered materials derived from eolian, alluvial, or colluvial deposits. It has weak to moderate alteration of the original material, with low clay and organic matter content, making it susceptible to erosion. While suitable for agriculture, its use is limited by topography, soil depth, and distribution in steeply sloped areas, where pine and oak forests are found (INEGI, 2014).

The distribution of described soil type within the aquifer is linked to vegetation and groundwater recharge and discharge zones (Cherry &

Freeze, 1979; Toth, 1959; Escolero-Fuentes, 2018). Natural grasslands thrive in saline soils, while mesquite forests grow in alluvial soils found in valleys and depressions, where the water table is near the surface (Fagundo-Castillo *et al*., 2014).

Physiography

The Cuauhtémoc aquifer is in the Physiographic Province of the Sierra Madre Occidental, within the sub provinces of the Tarahumara Mountain Ranges and Plains and the Durango Mountain Ranges and Plains (INEGI, 2010). The *Sierra Madre Occidental* Province starts in Nuevo León state and extends southeastward to Puebla and Veracruz states, where it joins to the Trans-Mexican Volcanic Belt. This mountainous system presents varied elevations, ranging from 500 to 3 600 masl. It is a Tertiary formation which began with the extrusion of large volumes of volcanic materials, with thicknesses ranging from 1 500 to 1 800 m. The Tarahumara Mountain Ranges and Plains subprovince covers the central-western portion of the state and is characterized by mountain ranges oriented North-South, separated by valleys and plains (INEGI, 1999). At the southeastern extreme an elevation of 2 200 masl, is the plain that houses Bustillos Lagoon (INEGI, 1999). This Subprovince is distinguished by a succession of expansive and elongated plains, separated by volcanic mountain ranges. The average elevation of the plains and mountains is 2 000 and 2 400 meters above sea level, respectively. The Durango Mountain Ranges and Plains subprovince is located near Cuauhtémoc and shows narrow plains at an altitude of 1 500 masl, along with valleys, chains of small mountain ranges, plateaus, and hills (SGM, 2005).

Tecnología y ciencias del agua, ISSN 2007-2422, 17(5), 433-477. DOI: 10.24850/j-tyca-2026-05-10

Regarding topography, the alluvial plain with rolling hills extends over most of the aquifer area. This landform suggests a flat terrain influenced by alluvial sedimentation processes (INEGI, 2010). Present to a lesser extent the rolling hills with gentle slopes indicate areas with undulating terrain surface and soft inclines or descents (INEGI, 1999). This configuration influences the direction of surface flow and has implications for aquifer recharge process (INEGI, 2010). Other landforms in the aquifer include high mountain ranges and rolling hills with plateaus (INEGI, 2010).

Hydrogeology

Previous studies indicate the presence of an unconfined, heterogeneous, and anisotropic aquifer (Conagua, 2023a). This aquifer consists of fractured and granular mediums, with hydraulic interconnection among them. The upper layer is formed by alluvial sediments of varying sizes, clayey sediments, and conglomerates, while the lower one consists of volcanic and sedimentary rocks with secondary permeability due to fractures. The thickness of the upper layer exceeds 350 m and increases toward the center of the valley (Conagua, 2023a). At greater depths, the limestones and sandstones form a semi-confined aquifer, as they are superimposed and alternated with shales and siltstones (Conagua, 2020). The aquifer is characterized by a complex regional geology that includes sedimentary rocks (sandstones, shales, limestones, and conglomerates), igneous rocks (granites, ignimbrites, andesites, rhyolites), and metamorphic rocks, as well as evaporitic, alluvial, lacustrine, and semi-consolidated deposits. Its age ranges from the Paleozoic to the

Tecnología y ciencias del agua, ISSN 2007-2422, 17(5), 433-477. DOI: 10.24850/j-tyca-2026-05-10

Quaternary with the presence of anticlines and synclines (SGM, 1997; SGM, 2002; SGM, 2005).

Regarding piezometry, in 2013 the static groundwater level ranged from 30 to 210 m. The shallowest depths (30 to 50 m) were found around Bustillos Lagoon, increasing as the terrain ascended toward the mountains that limit the aquifer. The deepest measurements (120 to 210 m) were recorded to the northeast of the aquifer. In the main exploitation zone, to the north and northwest of Ciudad Cuauhtémoc, the depth to the groundwater was 60 to 100 m (Conagua, 2020).

The groundwater flow network displays a concentric pattern toward the main area of Bustillos Lagoon. In the central region there is an extensive cone of depression encompassing the agricultural exploitation area (Conagua, 2020). From 2001 to 2013, the static level dropped by 5 to 40 m (Conagua, 2020). Groundwater extraction by 1997 was in the order of 183.2 hm^3/year (Conagua, 2015), and even there was a groundwater volume of 307.1 hm^3/year in the Water Rights Public Registry by 2022, increased notably to 497.9 hm^3/year (Conagua, 2023a). Groundwater decline level distributed in aquifer area shows as cones of depression generated mainly by extraction for agriculture use in aquifer area and locally around Cuauthémoc city due potable water supply pumping (Conagua, 2020). Even irrigated agriculture is for far, the main groundwater user sector with 95.9 % of total extraction, around 3.9 % is used for drinking water supply and the last portion for industrial and other minority uses like livestock (Conagua, 2024).

Materials and methods

Clip overlay tool and pattern analysis

Analysis tools and geoprocessing in ArcGIS vary across disciplines (Chang, 2022). For this research, Clip tool (Spatial Analyst Tool) was used to obtain and Calculate Geometry to assess LULC in the Cuauhtémoc Aquifer, Chihuahua, Mexico. The analysis was conducted using vector data, which represents spatial entities through points and X, Y coordinates. These entities serve as inputs for vector-based spatial analysis, meaning the accuracy of the results is directly influenced by the precision of their location and shape (Heywood *et al*., 2010).

Clip (an overlay analytical tool) was the first step used in this study as it enables the combination of spatial geometries and attribute tables. This overlay operation integrates geometries and attributes from multiple layers to generate a new dataset. While ArcMap allows overlay operations with multiple layers, this research focused on the intersection of two layers. The resulting geometry represents the spatial intersection of the input entities or layers (Chang, 2022), and the output dataset retains a combination of attributes from both inputs.

For accurate analysis, the overlapping entity layers must be spatially registered and share the same coordinate system. In this study all layers were referenced to the Universal Transverse Mercator (UTM) coordinate system, 13N zone, using the WGS84 ellipsoid and WGS84 horizontal datum, ensuring consistency in spatial alignment. The spatial data was defined by the Greenwich Prime Meridian and used degrees as the angular unit.

Tecnología y ciencias del agua, ISSN 2007-2422, 17(5), 433-477. DOI: 10.24850/j-tyca-2026-05-10

The ArcMap tool overlaying capacity involves two or more polygon layers and uses the Boolean connectors AND, OR, and XOR. In this case the Clip tool uses the AND connector (Slocum *et al*., 2023). To distinguish between layers, the LULC polygon layer was called the input layer, and the Cuauhtémoc Aquifer layer was called the overlay layer. The output combines the polygon boundaries of the input and overlay layers to create a result layer with attributes from both shapes (a new set of polygons called the LULC layer of the Cuauhtémoc Aquifer polygon). This result layer carries attributes from the original layers, which may differ from the attributes of the original polygons (Chang, 2022).

A pattern analysis was also conducted, which is the spatial arrangement of polygon features in a two-dimensional space. It utilizes measurements of distance and area as inputs and spatial statistics to describe the distribution (Slocum *et al*., 2023). On a global level a pattern analysis can reveal whether a distribution pattern is random, dispersed, or clustered. On a local level a pattern analysis can detect if a distribution pattern contains local clusters of high or low values. Since pattern analysis can be a precursor to a more structured data analysis, some studies consider this type of analysis as an activity of data exploration (Chang, 2022).

Results

Vector data sources

The Shapes were created by INEGI and downloaded from the web (G-Conabio, 2026), with a scale of 1:250 000. The data (downloaded in January 2025) contains spatial information on LULC, obtained through photointerpretation techniques using Landsat imagery and fieldwork (INEGI, 2023). These Shapes contain information on the location, distribution, and extent of plant communities and agricultural uses, with variations in vegetation types, crops, and relevant ecological information. This digital geographic information includes vector data encoded according to the "Vector data dictionary of LULC" applicable to different ecological units, plant communities, and anthropogenic uses (INEGI, 2023).

As complementary information, the table downloaded shows the following attributes: area, perimeter, and 16 types of LULC. These 16 types are classified based on their ecological affinity and floristic composition as follows: 1) Vegetation transition state according to changes in the vegetation cover (primary or secondary vegetation); 2) distribution of vegetation communities (based on variants such as ecological, floristic, and physiognomic elements), and 3) types of agriculture classified by water availability during the agricultural cycle and the duration of the cultivation cycle (INEGI, 2023).

For parsimonious principle, the 16 LULC were unified into the following 13 parameters: 1) Irrigated agriculture (annual irrigated agriculture + annual and permanent irrigated agriculture + permanent agricultural plantation irrigated agriculture); 2) rainfed agriculture; 3) oak forest; 4) oak-pine forest; 5) pine (*Pinus* in some varieties) (INEGI, 2017) forest; 6) pine-oak (*Quercus* in some varieties) (INEGI, 2017) forest; 7) water bodies (lakes, perennial and intermittent streams); 8) induced grassland; 9) natural grassland; 10) secondary shrub vegetation of oak forest; 11) secondary shrub vegetation of oak-pine forest; 12) secondary shrub vegetation of pine-oak forest); 13) urban area (human settlements + urban area).

One of the main advantages of using information provided by INEGI is that it is freely available, and benefits from continuous improvements in its processes. In addition, the classification of units is standardized and supported by interpretation manuals that are frequently updated.

Calculation of areas and evolution of LULC

The Calculate Geometry tool allows the determination of the geometry of entities in a layer (Chang, 2022). This tool can compute values such as area, perimeter, and coordinates, depending on the geometry of the input layer (points, polylines, or polygons). These values can only be calculated if the coordinate system is projected, and due to its versatility, the Calculate Geometry tool is one of the most widely used in ArcMap. Thus, the geometry of the resulting layer (referred to as the LULC Layer of the Cuauhtémoc Aquifer) was calculated, yielding various values for the entities (polygons). By this procedure, a resulting Table 1 was organized by total surface area and percentage of the aquifer, corresponding to LULC series I to VII from 1997 to 2021, respectively (Table 1); Figure 2 with graphical patterns and seven maps for LULC for each of the same years was also generated (Figure 3).

Table 1. Evolution of LULC by total area and percentage in the Cuauhtémoc aquifer (1997-2017).

LULC	Total area in km² (series I, 1997)	Total area in km² (series II, 2001)	Total area in km² (series III, 2005)	Total area in km² (series IV, 2009)	Total area in km² (series V, 2013)	Total area in km² (series VI, 2017)	Total area in km² (series VII, 2021)
Irrigated agriculture (IA)	36.25 (1.06 %)	818.73 (24.00 %)	1050.39 (30.79 %)	1080.89 (31.68 %)	996.28 (29.20 %)	1039.42 (30.47 %)	1016.19 (29.79 %)
Rainfed agriculture (RA)	1672.64 (49.03 %)	1010.06 (29.61 %)	841.93 (24.68 %)	843.31 (24.72 %)	821.83 (24.09 %)	775.64 (22.74 %)	740.27 (21.70 %)
Oak forest (OF)	116.85 (3.42 %)	105.51 (3.09 %)	97.07 (2.84 %)	100.11 (2.93 %)	100.11 (2.93 %)	100.11 (2.93 %)	104.88 (3.07 %)
Oak-pine forest (O-PF)	733.64 (21.50 %)	404.78 (11.86 %)	646.71 (18.96 %)	643.79 (18.87 %)	645.34 (18.92 %)	645.61 (18.92 %)	670.95 (19.67 %)
Pine forest (PF)	4.11 (0.12 %)	4.34 (0.12 %)	4.34 (0.12 %)	4.34 (0.12 %)	4.34 (0.12 %)	4.34 (0.12 %)	4.34 (0.12 %)
Pine-oak forest (P-OF)	187.19 (5.48 %)	217.42 (6.37 %)	192.12 (5.63 %)	192.19 (5.63 %)	192.17 (5.63 %)	196.11 (5.74 %)	197.47 (5.78 %)
Water bodies (WB)	96.59 (2.83 %)	150.60 (4.41 %)	101.72 (2.98 %)	102.97 (3.01 %)	102.99 (3.01 %)	102.72 (3.011 %)	140.70 (4.12 %)
Induced grassland (IG)	298.03 (8.73 %)	218.85 (6.41 %)	258.15 (7.56 %)	250.63 (7.34 %)	248.16 (7.27 %)	245.26 (7.19 %)	209.26 (6.13 %)
Natural grassland (NG)	214.89 (6.30 %)	398.55 (11.68 %)	86.46 (2.53 %)	60.79 (1.78 %)	58.31 (1.70 %)	51.22 (1.50 %)	66.04 (1.93 %)
Secondary shrub vegetation of oak forest (SSV-OF)	34.57 (1.01 %)	32.66 (0.95 %)	35.30 (1.03 %)	32.31 (0.94 %)	32.32 (0.94 %)	32.32 (0.94 %)	28.40 (0.83 %)
Secondary shrub vegetation of oak-pine forest (SSVO-PF)	13.62 (0.39 %)	11.85 (0.34 %)	25.73 (0.75 %)	27.58 (0.80 %)	27.58 (0.80 %)	27.58 (0.80 %)	35.21 (1.03 %)
Secondary shrub vegetation of pine-oak forest (SSVP-OF)	0.01 (0.01 %)	10.26 (0.30 %)	31.23 (0.91 %)	30.98 (0.90 %)	30.97 (0.90 %)	32.09 (0.94 %)	32.43 (0.95 %)
Urban area (UA)	2.40 (0.070 %)	27.21 (0.79 %)	39.68 (1.16 %)	40.91 (1.19 %)	150.41 (4.40 %)	158.37 (4.64 %)	164.71 (4.82 %)

Tecnología y Ciencias del Agua

OPEN ACCESS

Check for updates

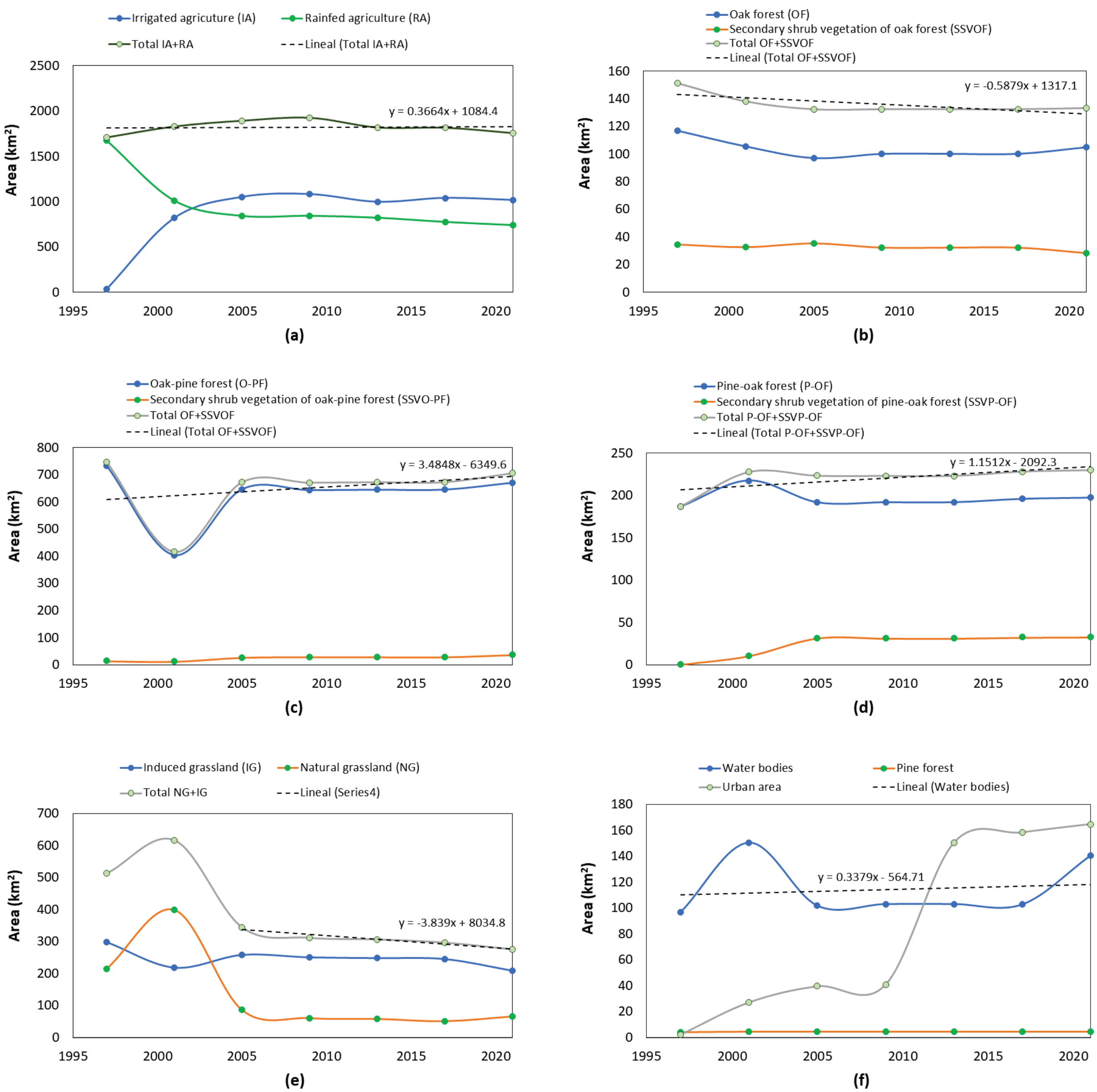

Figure 2. Evolution of LULC coverages: (a) IA, RA and IA+RA, (b) OF, SSV-OF and PF+SSV-OF, (c) O-PF, SSVO-PF and O-PF+SSVO-PF, (d) P-OF, SSVP-OF and P-OF+SSVP-OF, (e) IG, NG and IG+NG and (f) WB, PF and UA.

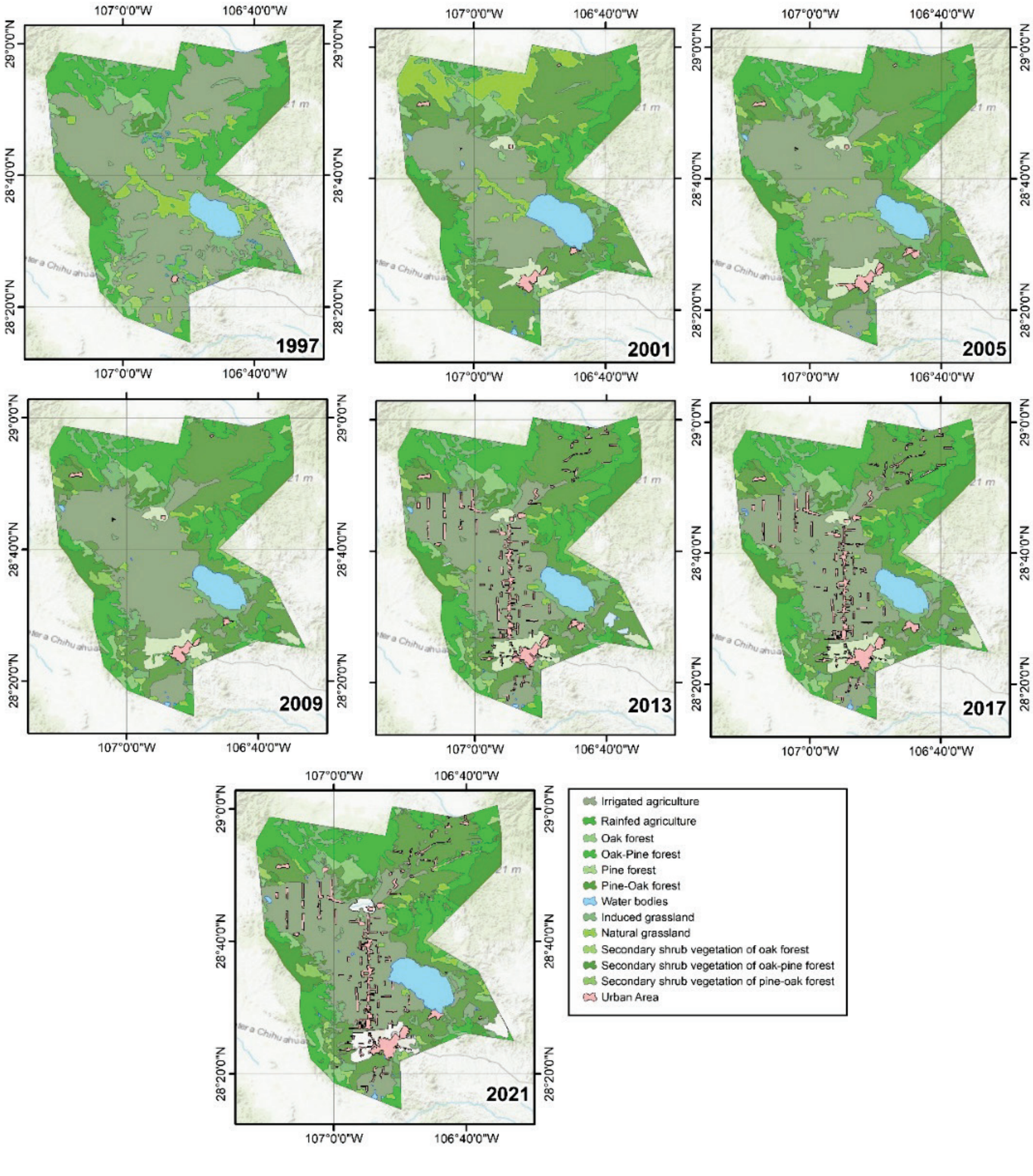

Figure 3. LULC spatial and temporal distribution in Cuauhtémoc Aquifer surficial polygon (Series I-VII, 1997-2021) (constructed from G-Conabio, 2026; INEGI, 2025).

Figure 2 presents six panels (a-f) illustrating the spatiotemporal changes in LULC within the Cuauhtémoc aquifer from 1997 to 2021. Each graph displays individual trend lines for specific LULC categories, along with a dashed black line representing the total area of the grouped categories. A linear regression model (Equation (1)) is used to depict temporal trends:

$$Area = \Delta \mathrm{a} \cdot \mathrm{year} + \mathrm{Area}\ (t_0) \quad (1)$$

Where:

$Area$ = total area of the land cover (km²).

year = time (year-date).

Δa = annual land cover change rate (km^2/y), indicating increment (positive) or decrement (negative) and the average rate of change

$Area(t_0)$ = estimated total land cover at initial year (cero for regression model).

This approach enables a quantitative assessment of the magnitude and direction of land cover average changes over time. Total agriculture use (IA + RA) average area observed a mean annual increment in the order of 0.37 km^2/y from 1997 to 2021; about 8.9 km^2 in the period. It is notorious that groundwater irrigated agriculture increased from 36.25 km^2 in 1997 to 818.73 km^2 in 2001, finishing in 1016.19 km^2 in 2021. As the time steps, rainfed agriculture decreased from 1 672.64 km^2 to 1 010.06 km^2, and finely to 740.27 km^2 at the end of the period.

Consequently, there were an additional 979.94 km^2, irrigated from groundwater in 2021, compare to 1997.

There was a conversion in agriculture practices possibly driven by the higher productivity yield necessity or by possible changes in the climate that made the agriculture rainfed labor harder. In relation to urban areas, calculations revealed an increase of 162.31 km^2, which may be attributable to inconsistencies in the cartographic analysis process used over the time in the downloaded LULC series. This inference is supported by a comparative analysis using high-resolution satellite imagery from Google Earth.

Regarding the oak forests and oak-pine forests area covering the study area, there was a reduction in the period in the order of 11.97 km^2 and 62.69 km^2, respectively; this behavior could be linked to agricultural activities and urban expansion. Also, secondary vegetation of oak-pine forests (21.58 km^2) and pine-oak forests (32.42 km^2) increased, suggesting degradation of primary forest due to logging. Additionally, the area of natural grasslands decreased by 148.85 km^2 indicating a land-use change toward agriculture or urbanization. Moreover, secondary shrub vegetation of pine-oak forests increased by 32.42 km^2, possibly due to the change of primary same coverage, due low scale wood exploitation (increase of human activities).

Regarding the geographic distribution of LULC, a decrease in rainfed agricultural areas is observed in the central and southern regions of the aquifer, along with an increase in urban settlements in the central, northeast, northwest, and southern regions. There is a small expansion of pine-oak forest areas in the southeast (near Bustillos Lagoon), an increase in small water bodies in the center-east of study area, a reduction of induced grasslands in the northwest (near the aquifer boundary), and an increase in natural grasslands in the east (near Anáhuac).

Finally, water bodies increased by 44.11 km², which may be explained by the annually variation in the Bustillos Lagoon free surface area that shows a direct correlation with rainfall surface runoff, reflecting a hydrodynamic response of the lacustrine system to natural variations in rainfall and to climatic changes.

Discussion

In the 21st century, northern Mexico has experienced events such as drought and climate change that have impacted water availability and driven changes in LULC (Conagua, 2023b; Corrales-Suastegui *et al*., 2022; Murray-Tortarolo & Salgado, 2021; USDA, 2020). Consequently, the Cuauhtémoc aquifer is undergoing an increasingly pronounced annual groundwater deficit, indicative of intensive groundwater uses in last years (Conagua, 2023a). This overreliance on non-renewable groundwater reserves represents a critical challenge to the long-term sustainability of regional water resources. Total agricultural land area spawn from 1708.89 km^2 (2.12 % irrigated and 97.88 % rainfed) in 2021 to 1 756.46 km^2 in (57.86 % irrigated and 42.13 % rainfed) in 2021, as can be computed from data in Table 1. This notable change in groundwater irrigated agricultural land area, is related to the rising deficit reported by the National Water Commission (Conagua, by its Spanish acronym) which also can be found in scientific literature (Santos-Hernández *et al*., 2019).

Regarding LULC, irrigated agriculture, pine forest, pine-oak forest, water bodies, secondary shrub vegetation of oak-pine forest, secondary shrub vegetation of pine-oak forest and Urban area increased, while rainfed agriculture, oak forest, oak-pine forest, induced grassland, natural grassland and secondary shrub vegetation of oak forest decreased (Table 2).

Table 2. LULC evolution in the Cuauhtémoc Aquifer (1997-2017).

LULC	**Change (km^2)**	**Change (%)**
Irrigated agriculture (IA)	979.94	28.7
Rainfed agriculture (RA)	-932.36	-27.3
Oak forest (OF)	-11.97	-0.4
Oak-pine forest (O-PF)	-62.69	-1.8
Pine forest (PF)	0.23	0.0
Pine-oak forest (POF)	10.23	0.3
Water bodies (WB)	44.11	1.3
Induced grassland (IG)	-88.77	-2.6
Natural grassland (NG)	-148.85	-4.4
Secondary shrub vegetation of oak forest (SSVO-F)	-6.16	-0.2
Secondary shrub vegetation of oak-pine forest (SSVOP-F)	21.58	0.6
Secondary shrub vegetation of pine-oak forest (SSVP-OF)	32.42	1.0
Urban area (UA)	162.31	4.8

These changes are driven by multiple interacting factors, including erosion, deforestation, population growth, wildfires, rising agricultural costs, drought, and climate change. Vegetation is categorized according to its water source: *phreatophytes*, which access water directly from the water table; *halophytes*, which thrive in areas where groundwater naturally discharges at the surface; *crops*, which rely on irrigation from pumped groundwater and surface water; and *xerophytes*, which obtain moisture primarily from precipitation and infiltration near the ground surface.

The results of this investigation are valuable for identifying zones of recharge and discharge within the aquifer, as different types of vegetation have distinct water demands (Escolero-Fuentes, 2018; Toth, 1959).

In the Cuauhtémoc aquifer, pine forest coverage increased in the surrounding hills and mountainous areas between 1997 and 2021, aligning with the aquifer's identified recharge zones. Over the same period, irrigated agriculture also expanded in the valley areas near Bustillos Lagoon, corresponding to discharge zones. These findings are consistent with previous studies that delineate recharge areas (Healy & Scanlon, 2010; Hogan *et al*., 2004; Sharma, 1989). Research conducted in various arid regions has shown that aquifer recharge typically occurs in mountainous zones, along intermittent stream channels, and in fractured bedrock areas-environments where grasslands commonly develop (Asano, 1985; Gale & Dillon, 2005; Healy & Scanlon, 2010; Sharma, 1989).

The results also correlate with the population growth in the region. The 4.8 % increase in urban settlements can be explained by population growth in recent years. In 2000, Cuauhtémoc population municipality was 135 586 inhabitants, which grew to 180 638 by 2020 (CIES, 2023; INEGI, 2010; INEGI, 2015).

Despite the existence of laws related to human settlements, territorial planning, and urban development at national and state level (DOF, 2024; POE, 2021), their implementation, as in many other laws even at international level, refers to a lag time. In Cuauhtémoc —like other municipalities in Mexico— agricultural and urban land has placed increasing pressure on both surface and groundwater resources. As a result, no additional volume is available for new concessions in terms of article 22th of the National Water Law (DOF, 2025), since the aquifer currently presents 7.75 hm^3/year deficit (DOF, 2023). Although partial legal restrictions to allow new groundwater extraction permissions have been in place since more than 60 years (DOF, 1957), the deficit has continued to increase from the twentieth century to nowadays. The two groundwater decrees limiting new groundwater extraction permissions —published on January 30, 1957 (DOF, 1957), and on October 21, 1967 (DOF, 1967)— stablishes that groundwater extraction can be only authorized for domestic purposes.

GIS analyses of LULC change can be utilized for multiple purposes, such as analyzing population growth, changes in agricultural activities, patterns of hydrological expansion or reduction, and identifying recharge and discharge zones of an aquifer. In the case of the Cuauhtémoc aquifer, the GIS analysis was useful to determine changes in vegetation coverage over the time, due to anthropogenic activities as well as due changes in climate.

Overall, the most significant LULC changes observed in the study area include the steady expansion of irrigated agriculture and urban areas, which suggests increased anthropogenic pressure and investment in infrastructure over time. Concurrently, a notable decline in induced grassland and oak forest cover points to ongoing land conversion processes.

In contrast, pine forests and secondary shrub vegetation associated with oak forest, oak-pine forest, and pine-oak forest experienced a decrease of less than 1 % over the study period. This minimal change suggests that these areas may have remained relatively stable due to limited accessibility and, consequently, reduced pressure for land-use transformation. The observed trends are supported by linear regression models, which reveal consistent patterns of growth or decline and offer valuable insight into future landscape dynamics (Figure 2).

Although the observed changes in LULC in the Cuauhtémoc aquifer show clear trends, the significant surface increase in urban settlements stand out. This can be attributed to inconsistencies in the data series, as in Series I (1997), the town of Anáhuac and the Mennonite fields do not appear. Additionally, agricultural areas were accounted for differently in Series I and II, which could explain the significant increase in irrigated agricultural land from 1997 to 2021. Another noteworthy issue is that none of the series include roads or highways, which could affect the calculation of urban area surfaces.

Therefore, it is recommended to validate the results using through field observations, an evaluation and the application of consistent methodologies across all temporal series, and the use of remote sensing techniques.

These changes reflected a transformation process largely driven by agricultural intensification and urban expansion-factors that may significantly impact groundwater availability in the Cuauhtémoc aquifer. The reduction of natural vegetation cover, combined with rising water demand, underscores the urgent need for sustainable management strategies that reconcile socioeconomic development with the preservation and efficient use of water resources.

Conclusions

This study evaluated LULC changes in the Cuauhtémoc aquifer between 1997 and 2021. The results revealed transformations particularly in the agricultural sector, with a decrease in rainfed agriculture and an increase in groundwater irrigated land. This shift has contributed to the notorious increment of groundwater extraction, in the order of 2.7 times from 1997 to 2022 as reported in Conagua technical studies, placing additional pressure on the aquifer. Furthermore, the population increase from 2000 to 2020, of 45 052 inhabitants, progressively demanded an additional volume of groundwater for human consumption, services and other socio-economic activities in urban and rural population centers.

Because of this, it is crucial to implement measures that establish pumping control mechanisms related to agricultural expansion. Without such regulations, the aquifer is likely to experience further deterioration. The main recommendations are to avoid excessive growth of the agricultural frontier, to increase groundwater use efficiency, and to reduce groundwater pumping.

The NWL regulates the water use to prevent over exploitation due mechanisms as: 1) Sustainable development, 2) mandatory water use planning, 3) denial of new concessions if applicable, 4) establishment of protected zones, and 5) regulation of land and water use, wish also helps to regulate land development and territory extensive human activities.

Another key finding is the degradation of primary forest cover, which compromises the aquifer's natural recharge capacity. At the same time, the expansion of the cropland in discharge zones, accelerating groundwater depletion. These dynamics threaten the long- term sustainability of the aquifer.

Additionally, cartographic inconsistencies were observed in the LULC datasets, highlighting the need for careful validation of geospatial data. The use of other methodologies like remote sensing possibly combined with LULC datasets is an area of opportunity to apply in future research, to assess physic evolution in hydrological systems.

The study highlights the urgency of adopting sustainable practices, such as crop rotation; contour plowing and the use of vegetative barriers on sloped terrain; protection of native vegetation; and the construction of gabion dams in intermittent channels feeding Bustillos Lagoon. Reforestation of headwater basins with native species is also essential to promote infiltration and restore ecological balance.

Unsustainable LULC practices —such as unregulated irrigation, poor drainage, overgrazing, and deforestation— are drivers of land degradation in arid and semi-arid regions globally. Future research should focus on identifying basin management techniques to mitigate hydrological change, including delineation of suitable areas for reforestation and the recognition of vulnerable zones for aquifer recharge. In addition, studies need to address the quantitative relationship between LULC changes and aquifer recharge, as well as assess the effectiveness of current land management policies. Strengthening local planning with reliable geospatial information is essential to reverse degradation trends and to support sustainable development in northern Mexico.

Finally, the methodology presented in this research uses public domain cartography available wide nation, that is actualized systematically and maintained by INEGI throughout the time, attributes that allows to consider it generalized and with the potential to be applied in other aquifers, watersheds, administrative regions or other managements units, to support making decision process regarding natural resources management (including water), land regulations and other related issues.

Acknowledgments

The authors would like to express their gratitude to the anonymous reviewers and editors for their valuable comments and suggestions. They also thank the Faculty of Engineering, Autonomous University of Chihuahua for the institutional support providing an adequate academic environment for the development of this article.

Funding

The authors declare that no funding support was received for the preparation of this article.

Statement on conflicts of interest

The authors declare no conflict of interest.

Statement on the use of AI

The authors declare that no Artificial Intelligence tools were used in the preparation of this article.

References

Alatorre, L. C., Granados, A., Bravo, L. C., Torres, M. E., Wiebe, L. C., Uc, M. I., González, M. O., Sánchez, E., Rojas, H. L., & Salas, V. (2019). Agricultural furrow irrigation inefficiency in the basin of Bustillos Lagoon, Chihuahua, Mexico: Geometric characteristics of agricultural plots and aquifer depletion. *Tecnología y ciencias del agua*, *10*(5), 241-281. https://doi.org/10.24850/j-tyca-2019-05-10

Antonakos, A., & Lambrakis, N. (2021). Spatial interpolation for the distribution of groundwater level in an area of complex geology using widely available GIS tools. *Environmental Processes*, *8*(3), 993-1026. https://doi.org/10.1007/s40710-021-00529-9

Arif, M., Sengupta, S., Mohinuddin, S. K., & Gupta, K. (2023). Dynamics of land use and land cover change in peri urban area of Burdwan city, India: A remote sensing and GIS based approach. *GeoJournal*, *88*(4), 4189-4213. https://doi.org/10.1007/s10708-023-10860-3

Asano, T. (1985). *Artificial recharge of groundwater*. Butterworth Publishers. https://doi.org/10.1016/C2013-0-03913-8

Balogun, I. A., Adeyewa, D. Z., Balogun, A. A., & Morakinyo, T. E. (2011). Analysis of urban expansion and land use changes in Akure, Nigeria, using remote sensing and geographic information system (GIS) techniques. *Journal of Geography and Regional Planning*, *4*(9), 533-541. https://academicjournals.org/journal/JGRP/article-abstract/E6F0E3740877

Bellia, F. F., & Lanfranco, S. (2019). A preliminary assessment of the efficiency of using drones in land cover mapping. *Xjenza Online*, *7*, 18-27. https://doi.org/10.7423/XJENZA.2019.1.02

Bravo-Peña, L. C., Sáenz-López, D. A., Alatorre-Cejudo, L. C., Priego-Santander, Á., Torres-Olave, M. E., & Granados-Olivas, A. (2016). Identificación de áreas potenciales de recarga hídrica en el acuífero Cuauhtémoc (Chihuahua) mediante una evaluación espacial multicriterio. In: *Estudios territoriales en México: percepción remota y sistemas de información espacial* (pp. 339-362). Universidad Autónoma de Ciudad Juárez. https://www.researchgate.net/publication/309118247_Identificacion_de_areas_potenciales_de_recarga_hidrica_en_el_acuifero_Cuauhtemoc_Chihuahua_mediante_una_evaluacion_espacial_multicriterio

Chang, K.-T. (2016). *Introduction to geographic information systems* (8th ed). McGraw Hill Education.

Chang, K.-T. (2022). *Introduction to geographic information systems* (10th ed). McGraw Hill.

Cherry, J. A., & Freeze, R. A. (1979). *Groundwater*. Prentice-Hall.

CIES, Centro de Información Económica y Social. (2023). *Perfil económico región Cuauhtémoc*. https://www.chihuahua.com.mx/content/PERFIL%20REGIONAL/2023/Región%20Cuauhtémoc.pdf

Conagua, Comisión Nacional del Agua. (2015). *Actualización de la disponibilidad media anual de agua en el acuífero Cuauhtémoc (0805), estado de Chihuahua*. https://www.gob.mx/cms/uploads/attachment/file/103566/DR_0805.pdf

Conagua, Comisión Nacional del Agua. (2020). *Actualización de la disponibilidad media anual de agua en el acuífero Cuauhtémoc (0805), estado de Chihuahua*. Comisión Nacional del Agua.

Conagua, Comisión Nacional del Agua. (2023a). *Actualización de la disponibilidad media anual de agua en el acuífero Cuauhtémoc (0805), estado de Chihuahua*. Comisión Nacional del Agua.

Conagua, Comisión Nacional del Agua. (2023b). *Estadísticas del agua en México*. https://sinav30.conagua.gob.mx:8080/port_publicaciones.html

Conagua, Comisión Nacional del Agua. (2024). *Actualización de la disponibilidad media anual de agua en el acuífero Cuauhtémoc (0805), estado de Chihuahua*. https://sigagis.Conagua.gob.mx/gas1/Edos_Acuiferos_18/chihuahua/DR_0805.pdf

Conagua, Comisión Nacional del Agua. (2026). *Disponibilidad en acuíferos*. https://sinav30.conagua.gob.mx:8080/SINA/?opcion=acuiferos

Corrales-Suastegui, A., Martinez-Diaz, G., Ruiz-Alvarez, O., Gonzalez-Gonzalez, M.A., Pavia, E. G. (2022). Temperature and precipitation towards the end of the 21st Century in pecan producing areas of Mexico. In: Rao, C. M., Patra, K. C., Jhajharia, D., & Kumari, S. (eds.). *Advanced modelling and innovations in water resources engineering. Lecture notes in Civil Engineering* (pp. 235-254). https://doi.org/10.1007/978-981-16-4629-4_17

Craig, J. R., Vaughan, D. J., & Skinner, B. J. (2013). *Earth resources and the environment*. Pearson New International Edition. https://books.google.co.uk/books?id=ijqpBwAAQBAJ

DOF, Diario Oficial de la Federación. (2023, noviembre 1). *Acuerdo por el que se actualiza la disponibilidad media anual de agua subterránea de los 653 acuíferos de los Estados Unidos Mexicanos, mismos que forman parte de las regiones hidrológico-administrativas que se indican de 2023*. https://www.dof.gob.mx/nota_detalle.php?codigo=5708074&fecha=09/11/2023

DOF, Diario Oficial de la Federación. (1957, enero 30). *Acuerdo que establece el Distrito de Riego de El Carmen, en San Buenaventura y Villa Ahumada, Chih., y declara de utilidad pública la construcción de las obras que lo formen y la adquisición de los terrenos necesarios para alojarlas y operarlas de 1957*. § Tomo CCXX-Núm. 25. https://www.dof.gob.mx/nota_to_imagen_fs.php?codnota=4461057&fecha=30/01/1957&cod_diario=188731

DOF, Diario Oficial de la Federación. (1967, octubre 21). *Decreto que establece veda por tiempo indefinido para el alumbramiento de agua del subsuelo en la zona conocida como región de Cuauhtémoc, del estado de Chihuahua* de 1967. § Tomo CCLXXXIV-Núm. 42. https://dof.gob.mx/nota_to_imagen_fs.php?codnota=4773448&fecha=21/10/1967&cod_diario=205579

DOF, Diario Oficial de la Federación. (2025, diciembre 11). *Ley de Aguas Nacionales de 1992*. www.diputados.gob.mx/LeyesBiblio/pdf/LAN.pdf

DOF, Diario Oficial de la Federación. (2024, abril 1). *Ley General de Asentamientos Humanos, Ordenamiento Territorial y Desarrollo Urbano de 2016*. www.diputados.gob.mx/LeyesBiblio/pdf/LGAHOTDU.pdf

Escolero-Fuentes, O. (2018). *Sistemas regionales de flujo de agua subterránea en México*. Instituto Mexicano de Tecnología del Agua. https://www.geologia.unam.mx/igl/docs/libros/Sistemas%20regionales%20de%20flujo.pdf

G-Conabio, Geoportal Conabio 2026. (2026). *Uso de suelo y vegetación escala 1:250,000. Series I a VII*. http://www.conabio.gob.mx/informacion/gis/

Fagundo-Castillo, J. R., Alconada-Magliano, M. M., Carrillo-Rivera, J. J., & González-Hernández, P. (2014). Caracterización de los flujos de agua subterránea a partir de su salinidad. *Tecnología y ciencias del agua*, *5*(3), 63-80. https://www.revistatyca.org.mx/index.php/tyca/article/view/428

Gale, I., & Dillon, P. (2005). *Strategies for managed aquifer recharge (MAR) in semi-arid areas*. https://unesdoc.unesco.org/ark:/48223/pf0000143819

García, E. (2004). *Modificaciones al sistema de clasificación climática de Köppen* (5ª ed). Universidad Nacional Autónoma de México. https://publicaciones.geografia.unam.mx/index.php/ig/catalog/book/83

Gavade, A. B., & Rajpurohit, V. S. (2021). Systematic analysis of satellite image-based land cover classification techniques: Literature review and challenges. *International Journal of Computers and Applications*, *43*(6), 514-523. https://doi.org/10.1080/1206212X.2019.1573946

Havlin, J. L., Tisdale, S. L., Nelson, W. L., & Beaton, J. D. (2017). *Soil fertility and fertilizers an introduction to nutrient management* (8th ed.). Pearson.

Healy, R., & Scanlon, B. (2010). *Estimating groundwater recharge*. Cambridge. https://doi.org/10.1017/CBO9780511780745

Heywood, I., Cornelius, S., & Carver, S. (2010). *An introduction to Geographical Information Systems* (3rd ed.). Pearson.

Hogan, J. F., Phillips, F. M., & Scanlon, B. R. (2004). *Groundwater recharge in a desert environment: The Southwestern United States*. https://doi.org/10.1029/WS009

Hussain, S., Mubeen, M., Akram, W., Ahmad, A., Habib-ur-Rahman, M., Ghaffar, A., Amin, A., Awais, M., Farid, H. U., Farooq, A., & Nasim, W. (2020). Study of land cover/land use changes using RS and GIS: A case study of Multan district, Pakistan. *Environmental Monitoring and Assessment*, *192*(1). https://doi.org/10.1007/s10661-019-7959-1

IMTA, Instituto Mexicano de Tecnología del Agua. (2015). *Atlas de la vulnerabilidad hídrica en México ante al cambio climático*. https://www.gob.mx/imta/documentos/atlas-de-vulnerabilidad-hidrica-en-mexico-ante-el-cambio-climatico-167655

INEGI, Instituto Nacional de Estadística y Geografía. (1999). *Estudio hidrológico del estado de Chihuahua*. INEGI. https://www.inegi.org.mx/contenidos/productos/prod_serv/contenidos/espanol/bvinegi/productos/historicos/2104/702825221768/702825221768_1.pdf

INEGI, Instituto Nacional de Estadística y Geografía. (2010). *Compendio de información geográfica municipal 2010 Cuauhtémoc Chihuahua*. https://www.inegi.org.mx/contenidos/app/mexicocifras/datos_geograficos/08/08017.pdf

INEGI, Instituto Nacional de Estadística y Geografía. (2014). *Guía para la interpretación de cartografía: edafología: escala 1:250,000: serie III*. https://www.inegi.org.mx/contenidos/productos/prod_serv/contenidos/espanol/bvinegi/productos/nueva_estruc/702825076221.pdf

INEGI, Instituto Nacional de Estadística y Geografía. (2015). *Las zonas metropolitanas en México*. https://www.inegi.org.mx/contenidos/programas/ce/2014/doc/minimonografias/m_zmm_ce2014.pdf

INEGI, Instituto Nacional de Estadística y Geografía. (2017). *Guía para la interpretación de cartografía: uso del suelo y vegetación: escala 1:250,000: serie VI*. https://www.inegi.org.mx/contenidos/productos/prod_serv/contenidos/espanol/bvinegi/productos/nueva_estruc/702825092030.pdf

INEGI, Instituto Nacional de Estadística y Geografía. (2023). *Diccionario de datos de uso de suelo y vegetación escala 1:250 000: versión 2*. Instituto Nacional de Estadística y Geografía. https://www.inegi.org.mx/contenidos/productos/prod_serv/contenidos/espanol/bvinegi/productos/nueva_estruc/889463908364.pdf

INEGI, Instituto Nacional de Estadística y Geografía. (2025). *Conjunto nacional de información topográfica a escala 1:50 000* (edición 2025, formato Shapefile) (conjunto de datos geoespaciales). https://www.inegi.org.mx/app/biblioteca/ficha.html?upc=794551163047

Keller, E. (2012). *Introduction to environmental geology* (5th ed). Pearson Prentice Hall.

López, E., Bocco, G., Mendoza, M., Velázquez, A., & Aguirre-Rivera, R. (2006). Peasant emigration and land-use change at the watershed level: A GIS-based approach in Central Mexico. *Agricultural Systems*, *90*(1-3), 62-78. https://doi.org/10.1016/j.agsy.2005.11.001

Medina-García, G., Ariel Ruiz-Corral, J., Rafael Ramírez-Legarreta, M., & Díaz Padilla, G. (2011). Efecto del cambio climático en la acumulación de frío en la región manzanera de Chihuahua. *Revista Mexicana de Ciencias Agrícolas*, *1*(1), 1-13. https://www.scielo.org.mx/scielo.php?script=sci_arttext&pid=S2007-09342011000800007

Montiel-González, C., García-Oliva, F., Bautista, F., & Sánchez-Meneses, O. (2021). The global climate change footprint in a Mexican desert ecosystem: The increasing frequency of extreme climatic events. *Tecnología y ciencias del agua*, *12*(4), 219-268. https://doi.org/10.24850/j-tyca-2021-04-05

Muhangane, L., & Andama, M. (2024). Modelling land use/land cover change of river Rwizi Catchment, South-Western Uganda using GIS and Markov chain model. *Journal of Water Resource and Protection*, *16*(02), 181-206. https://doi.org/10.4236/jwarp.2024.162011

Murray-Tortarolo, G. N., & Salgado, M. M. (2021). Drought as a driver of Mexico-US migration. *Climatic Change*, *164*(3-4). https://doi.org/10.1007/s10584-021-03030-2

Plaster, E. J. (2014). *Soil science & management* (6th ed). Cengage Learning.

Plieninger, T. (2006). Habitat loss, fragmentation, and alteration-Quantifying the impact of land-use changes on a Spanish dehesa landscape by use of aerial photography and GIS. *Landscape Ecology*, *21*(1), 91-105. https://doi.org/10.1007/s10980-005-8294-1

POE, Periódico Oficial del Estado. (2021, octubre 2). *Ley de Asentamientos Humanos, Ordenamiento Territorial y Desarrollo Urbano del estado de Chihuahua*. https://www.congresochihuahua2.gob.mx/biblioteca/leyes/archivosLeyes/1536.pdf

Santos-Hernández, A. L., Palacios-Velez, E., Mejía-Saenz, E., Matus-Gardea, J. A., Galvis-Spíndola, A., Vásquez-Soto, D., Ascencio-Hernández, R., & Peña-Díaz, S. A. (2019). Análisis del uso del agua del acuífero Cuauhtémoc, Chihuahua, México. *Tecnología y ciencias del agua*, *10*(3), 156-189. https://doi.org/10.24850/j-tyca-2019-03-07

SGM, Servicio Geológico Mexicano. (1997). *Carta geológico minera H13-10 "Chihuahua", escala 1:250,000*. https://mapserver.sgm.gob.mx/Cartas_Online/geologia/36_H13-10_GM.pdf

SGM, Servicio Geológico Mexicano. (2002). *Carta geológico minera H13-C85 "Tutuaca" escala 1:50,000* (Vol. 01). https://mapserver.sgm.gob.mx/Cartas_Online/geologia/682_H13-C85_GM.pdf

SGM, Servicio Geológico Mexicano. (2005). *Carta geológico-minera "Cusihuiriachic" 1:50,000 H13-C84*. https://mapserver.sgm.gob.mx/Cartas_Online/geologia/648_H13-C84_GM.pdf

Shalaby, A., & Tateishi, R. (2007). Remote sensing and GIS for mapping and monitoring land cover and land-use changes in the Northwestern coastal zone of Egypt. *Applied Geography*, *27*(1), 28-41. https://doi.org/10.1016/j.apgeog.2006.09.004

Sharma, M. L. (1989). *Groundwater recharge*. CRC Press.

Shrestha, S., Cui, S., Xu, L., Wang, L., Manandhar, B., & Ding, S. (2021). Impact of land use change due to urbanisation on surface runoff using GIS-based SCS–CN method: A case study of Xiamen City, China. *Land*, *10*(8). https://doi.org/10.3390/land10080839

Simental-Nájera, J. G., Arreguín-Cortés, F. I., Farfán-Gutiérrez, M., & Cervantes-Jaimes, C. E. (2023). Land use/land cover change and climate change impact on the hydrological response of El Rejón Dam watershed using artificial intelligence. *Tecnología y ciencias del agua*, *14*(4), 456-494. https://doi.org/10.24850/j-tyca-14-04-10

Slocum, T. A., McMaster, R. B., Kessler, F. C., & Hugh, H. (2023). *Thematic cartography and geovisualization*. https://doi.org/10.1201/9781003150527

SMN, Servicio Meteorológico Nacional. (2025). *Normales climatológicas por estado. Chihuahua*. https://smn.Conagua.gob.mx/es/climatologia/informacion-climatologica/normales-climatologicas-por-estado?estado=chih

Taratula, R., Kovalyshyn, O., Ryzhok, Z., & Malakhova, S. (2019). Application of mathematical modelling for optimization of land-use management. *Real Estate Management and Valuation*, *27*(3), 59-68. https://doi.org/10.2478/remav-2019-0025

Tarbuck, E. J., Lutgens, F. K., & Tasa, D. (2020). *Ciencias de la tierra. Una introducción a la geología física* (10th ed). Pearson.

Toth, J. (1959). *Gravitational systems of groundwater flow*. Cambridge

USDA, United States Department of Agriculture. (2020). *Sustainable water resources for irrigated agriculture in a desert river basin facing drought and competing demands: From characterization to solutions*. (Grant No. 2015-68007-23130). https://portal.nifa.usda.gov/web/crisprojectpages/1005789-sustainable-water-resources-for-irrigated-agriculture-in-a-desert-river-basin-facing-climate-change-and-competing-demands-from-characterization-to-solutions.html

UNESCO. (2022). Informe mundial de las Naciones Unidas sobre el desarrollo de los recursos hídricos 2022: aguas subterráneas: hacer visible el recurso invisible. UNESCO. https://unesdoc.unesco.org/ark:/48223/pf0000380726_spa

Utami, W., Sugiyanto, C., & Rahardjo, N. (2024). Artificial intelligence in land use prediction modeling: A review. *IAES International Journal of Artificial Intelligence*, *13*(3), 2514-2523. https://doi.org/10.11591/ijai.v13.i3.pp2514-2523

Villanueva-Hernández, H., Tovar-Cabañas, R., & Vargas-Castilleja, R. (2019). Classification of aquifers in the Mina field, Nuevo Leon, using geographic information systems. *Tecnología y ciencias del agua*, *10*(3), 96-121. https://doi.org/10.24850/j-tyca-2019-03-05

Weil, R. R., & Brady, N. C. (2016). *The nature and properties of soils* (15th ed.). Pearson.

Wiatkowska, B., Słodczyk, J., & Stokowska, A. (2021). Spatial-temporal land use and land cover changes in urban areas using remote sensing images and GIS analysis: The case study of Opole, Poland. *Geosciences (Switzerland)*, *11*(8). https://doi.org/10.3390/geosciences11080312

Xu, G., Su, X., Zhang, Y., & You, B. (2021). Identifying potential sites for artificial recharge in the plain area of the daqing river catchment using GIS-based multi-criteria analysis. *Sustainability (Switzerland)*, *13*(7). https://doi.org/10.3390/su13073978